

# Reconfigurable Intelligent Surface Enabled Spatial Multiplexing with Fully Convolutional Network

Bile Peng, *Member, IEEE*, Jan-Aike Termöhlen, *Student Member, IEEE*,  
Cong Sun, *Member, IEEE*, Danping He, *Member, IEEE*, Ke Guan, *Senior  
Member, IEEE*, Tim Fingscheidt, *Senior Member, IEEE*,  
and Eduard A. Jorswieck, *Fellow, IEEE*

## Abstract

Reconfigurable intelligent surface (RIS) is an emerging technology for future wireless communication systems. In this work, we consider downlink spatial multiplexing enabled by the RIS for weighted sum-rate (WSR) maximization. In the literature, most solutions use alternating gradient-based optimization, which has moderate performance, high complexity, and limited scalability. We propose to apply a fully convolutional network (FCN) to solve this problem, which was originally designed for semantic segmentation of images. The rectangular shape of the RIS and the spatial correlation of channels with adjacent RIS antennas due to the short distance between them encourage us to apply it for the RIS configuration. We design a set of channel features that includes both cascaded channels via the RIS and the direct channel. In the base station (BS), the differentiable minimum mean squared error (MMSE) precoder is used for pretraining and the weighted minimum mean squared error (WMMSE) precoder is then applied for fine-tuning, which is nondifferentiable, more complex, but achieves a better performance. Evaluation results show that the proposed solution has higher performance and allows for a faster evaluation than the baselines. Hence it scales better to a large number of antennas, advancing the RIS one step closer to practical deployment.

B. Peng, J. Termöhlen, T. Fingscheidt, and E. A. Jorswieck are with Institute for Communications Technology, TU Braunschweig, 38106 Braunschweig, Germany (e-mail: {b.peng,j.termoehlen,t.fingscheidt,e.jorswieck}@tu-braunschweig.de).

C. Sun is with Beijing University of Posts and Telecommunications, Beijing, China, 100876 (e-mail: suncong86@bupt.edu.cn).

D. He and K. Guan are with State Key Laboratory of Rail Traffic Control and Safety, Beijing Jiaotong University, Beijing, China, 100044 (e-mail: hedanping@bjtu.edu.cn, ke.guan.cn@ieee.org).

## Index Terms

Reconfigurable intelligent surface, weighted sum-rate maximization, fully convolutional network, weighted minimum mean squared error precoding.

## I. INTRODUCTION

The reconfigurable intelligent surface (RIS) is an emerging technology for next-generation wireless communication systems [1]–[5]. It comprises many antennas on a surface. Each antenna has the ability to receive a signal, process it without external power (i.e., the signal cannot be amplified), and reflect it. With cooperation between the antennas, the RIS can realize complicated signal processing. Due to its simple structure and good compatibility with the other components of wireless communication systems (e.g., precoding in the base station (BS)), the RIS is widely believed to be an essential part of the next-generation wireless communication systems and has been widely studied for optimizing weighted sum-rate (WSR) [6], [7], capacity [8], energy efficiency [9], reliability [10], physical layer security [11], [12] and wireless power transfer [13], [14].

Among different applications of the RIS, we focus on improving the WSR with spatial multiplexing in this work. The high data rate is a major challenge for future wireless communication systems, which can only be overcome by both acquiring broader bandwidth in higher frequencies and improving the spectrum efficiency. With a favorable propagation channel, we can use the same resource block (a resource allocation unit in time and frequency domains) to serve multiple users and hence improve the spectrum efficiency.

Without RIS, the propagation channel depends mainly on positions of transmitter and receivers and nearby scatterers, which we cannot optimize. If we deploy an RIS in the environment, we can optimize the environment by configuring the RIS such that the propagation channel is more favorable for spatial multiplexing.

This is a challenging problem because of its high dimensionality due to the large number of RIS antennas and the constraint that RIS does not amplify the signal. In the literature, the minimum mean squared error (MMSE) precoder [15] and the weighted minimum mean squared error (WMMSE) precoder [16] are proposed for precoding in the BS without consideration of the RIS, stochastic successive convex approximation [7], majorization-maximization [17], alternating optimization (AO) [18], and alternating direction method of multipliers (ADMM) [19] are applied to jointly optimize the RIS configuration and the BS precoding. These proposed

algorithms have achieved reasonable performance at the cost of high computational effort. With similar problem formulations, spatial multiplexing in RIS-assisted uplink is considered and a gradient-based solution is proposed [20]. The Riemannian manifold conjugate gradient (RMCG) and the Lagrangian method are applied to configure multiple RISs and BS to serve users on the cell edge [21]. A joint precoding scheme with an alternating optimization (AO) method is proposed for cell-free RIS-aided communication [8]. The sum-rate is maximized with the majorization-maximization (MM) algorithm for grouped users in a RIS-aided communication system [22]. The downlink signal-to-noise ratio (SNR) is maximized with deep reinforcement learning (DRL) [23]. The spectrum and energy efficiency are maximized with RIS [9], [24]. The interference caused by secondary networks is mitigated with an RIS [25]. The BS configuration and the phase shifts of the RIS are iteratively optimized with the orthogonal frequency-division multiplexing (OFDM) transmission scheme [26], [27]. The robust transmission scheme design is addressed as well [28].

Although the above-mentioned pioneering works have achieved reasonably good performances compared to random phase shifts and scenarios without RIS, there is still considerable room for performance improvement and the computational complexities of these proposed algorithms are still too high for real-time application. Besides, the high complexity constrains the number of RIS antennas. In most works mentioned above, the number of RIS antennas is assumed to be less than 200, which is far less than the vision of up to thousands of elements introduced in Ref. [4]. In recent years, there have been attempts to apply machine learning to RIS optimization for better scalability [29], [30].

In this work, we propose an approach based on fully convolutional network (FCN) and WMMSE precoding that achieves better performance with less operating expenses. The FCN is comprised of multiple convolutional layers and was first proposed in Ref. [31] for semantic segmentation, i.e., it takes an image as input and predicts the category of each pixel of the image (e.g., the car, the road, or the sky). The first convolutional layer is able to extract the local features of the image while the following convolutional layers can process information on higher levels. Inspired by the rectangular shape of the RIS and the spatial correlation of the channels of adjacent RIS antennas due to the close distance between the antennas [32], we apply an FCN for the RIS configuration. In the literature, the FCN has been applied to object detection [33], visual tracking [34] and receiver design [35]. To the authors' best knowledge, it has not yet been applied to RIS configuration.

Our contributions in this paper are as follows:

- We apply an FCN for the RIS configuration. We show that the FCN is an efficient and scalable architecture for the considered WSR maximization problem. By introducing dropout layers, we prevent overfitting and improve the generalization of the trained models.
- We design a trick to consider the direct channel without RIS in the FCN, which makes the proposed approach more applicable because a weak direct channel exists in most use cases.
- We design a training process with the WMMSE precoder, which is nondifferentiable and therefore incompatible with the gradient ascent optimization. By alternatingly training the FCN and updating the precoding vectors, the FCN can work properly with the WMMSE precoder.

In the following part of this work, Section II formulates the problem, Section III describes the precoding techniques, Section IV proposes our solution, Section V explains some issues of implementation and training, Section VI presents the training and evaluation results and Section VII concludes the work.

*Notations:* Throughout this work, we use the following notations:  $\mathbf{I}_n$  is an identity matrix of size  $n \times n$ ,  $\mathbf{0}_n$  is a zero matrix of size  $n \times n$ ,  $\mathbf{A} \star \mathbf{B}$  denotes the 2-dimensional cross-correlation between  $\mathbf{A}$  and  $\mathbf{B}$ ,  $|z|$  and  $\arg(z)$  are the amplitude and phase of complex number  $z$ , respectively,  $\mathbf{A}^+$  denotes the pseudoinverse of matrix  $\mathbf{A}$ ,  $\bar{\theta}$  refers to the untrainable neural network parameter set  $\theta$  (i.e., it is considered constant during training),  $\exp(\mathbf{A})$  is the elementwise exponential function.

## II. PROBLEM FORMULATION

We consider an RIS-aided communication with direct propagation path between BS and users. Our objective is to serve two users with the same resource block and to maximize the WSR of the two users. The BS is assumed to have multiple antennas and can do precoding subject to the transmit power constraint  $E_{Tr}$ . The RIS is assumed to be rectangular with  $H$  rows and  $W$  columns of antennas. Each RIS antenna has the ability to receive signal, adjust its complex phase without changing its amplitude and transmit it.

We denote the precoding matrix as  $\mathbf{V}$  of size  $M \times 2$ , where  $M$  is the number of BS antennas, the channel from BS to RIS as  $\mathbf{H}$  of size  $N \times M$ , where  $N$  is the number of RIS antennas ( $N = WH$ ) and element  $h_{nm}$  in row  $n$  and column  $m$  represents the channel gain from the  $m$ th antenna of the BS to the  $n$ th antenna of the RIS. The RIS signal processing is denoted by the

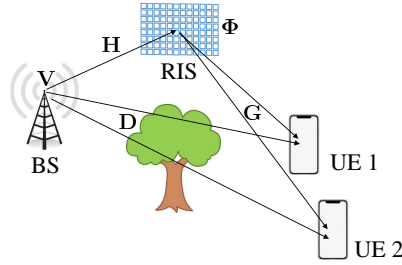


Fig. 1. System model.

diagonal matrix  $\Phi$  of size  $N \times N$ , where the element  $\phi_{nn}$  in row  $n$  and column  $n$  is  $e^{j\psi_n}$ , with  $\psi_n$  being the phase shift of antenna  $n$ . The channel matrix from RIS to users is denoted as  $\mathbf{G}$  of size  $2 \times N$ , where the element  $g_{un}$  denotes the channel gain from RIS antenna  $n$  to user  $u$ . The direct channel from BS to users is denoted as  $\mathbf{D}$  of size  $2 \times M$ , where the element  $d_{um}$  in row  $u$  and column  $m$  is the channel gain from the  $m$ th BS antenna to the  $u$ th user, the transmission is described as

$$\mathbf{y} = (\mathbf{G}\Phi\mathbf{H} + \mathbf{D})\mathbf{V}\mathbf{x} + \mathbf{n}, \quad (1)$$

where  $\mathbf{x}$  is the vector of transmitted symbols,  $\mathbf{y}$  is the vector of received symbols and  $\mathbf{n}$  is the vector of thermal noise. All three vectors have the same size<sup>1</sup> of  $2 \times 1$ . The whole system model is illustrated in Fig. 1.

Let

$$\mathbf{C} = (\mathbf{G}\Phi\mathbf{H} + \mathbf{D})\mathbf{V} \quad (2)$$

and  $c_{ij}$  being the element of  $\mathbf{C}$  in row  $i$  and column  $j$ , the objective is to maximize the WSR. Therefore, the problem can be formulated as

$$\begin{aligned} \max_{\mathbf{V}, \Phi} \quad & f = \alpha_1 \log_2 \left( 1 + \frac{c_{11}}{c_{12} + \frac{1}{\rho}} \right) + \alpha_2 \log_2 \left( 1 + \frac{c_{22}}{c_{21} + \frac{1}{\rho}} \right) \\ \text{s.t.} \quad & \text{tr}(\mathbf{V}\mathbf{V}^H) \leq E_{Tr} \\ & |\phi_{nn}| = 1 \\ & |\phi_{nn'}| = 0 \text{ for } n \neq n', \end{aligned} \quad (3)$$

<sup>1</sup>We assume two users in this work. However, the proposed method can be easily extended to more than two users by stacking user channels in  $\mathbf{G}$  and  $\mathbf{D}$ .

where  $\alpha_1$  and  $\alpha_2$  are weights of user 1 and user 2, respectively,  $\alpha_1, \alpha_2 \in [0, 1]$  and  $\alpha_1 + \alpha_2 = 1$ , and  $\rho$  is the transmit signal-to-noise ratio (TSNR), which is the ratio between transmit power and noise power.

### III. THE MMSE AND WMMSE PRECODER

In problem (3),  $\mathbf{H}$ ,  $\mathbf{G}$  and  $\mathbf{D}$  are given and we would like to optimize both  $\mathbf{V}$  and  $\Phi$ . While the RIS optimization problem (i.e., optimizing  $\Phi$ ) is new, the precoding problem (i.e., optimizing  $\mathbf{V}$ ) has been intensively studied in the literature. Different precoding techniques, such as maximum ratio transmission (MRT), zero-forcing (ZF), MMSE and WMMSE are proposed. Among them, the MMSE precoder can minimize the mean squared error caused by both interference and noise with a closed form solution and is the optimal precoder for a single user [15]. Furthermore, the iterative WMMSE precoder introduces weights of the mean squared errors (MSEs) of different users in the multi-user multiple-input-multiple-output (MIMO) system. It is proven that minimizing the sum of weighted MSEs for certain weights is equivalent to maximizing the WSR [16]. However, the WMMSE precoder does not have a closed-form solution and is only available as an iterative algorithm, which significantly increases its complexity compared to the MMSE precoder. Accordingly we cannot compute its derivative. In the following, we briefly introduce the two precoders that will be applied jointly with the RIS optimization.

#### A. The MMSE Precoder

In the MMSE precoder, the error is defined as the difference between transmitted symbols  $\mathbf{x}$  and received symbols  $\mathbf{y}$  scaled by a proper factor  $\beta^{-1}$  (because the received symbols are weaker due to the propagation loss). Accordingly, the MSE is defined as

$$\begin{aligned} \mathbf{e} &= \mathbb{E}(\|\beta^{-1}\mathbf{y} - \mathbf{x}\|_2^2) \\ &= \mathbb{E}(\|\beta^{-1}(\mathbf{C}\mathbf{V}\mathbf{x} + \mathbf{n}) - \mathbf{x}\|_2^2). \end{aligned} \quad (4)$$

The objective is to minimize the MSE subject to the transmit power constraint:

$$\begin{aligned} \min_{\beta, \mathbf{V}} \quad & \mathbb{E}(\|\beta^{-1}(\mathbf{C}\mathbf{V}\mathbf{x} + \mathbf{n}) - \mathbf{x}\|_2^2) \\ \text{s.t.} \quad & \text{tr}(\mathbf{V}\mathbf{V}^H) \leq E_{Tr}. \end{aligned} \quad (5)$$

When we assume  $\mathbb{E}(\mathbf{x} \cdot \mathbf{x}^T) = \mathbf{I}_2$ ,  $\mathbb{E}(\mathbf{n} \cdot \mathbf{n}^T) = 1/\rho \cdot \mathbf{I}_2$  and  $\mathbb{E}(\mathbf{n} \cdot \mathbf{x}^T) = \mathbf{0}_2$ , we obtain a closed-form solution [15]

$$\mathbf{V} = \beta \left( \mathbf{C}^H \mathbf{C} + \frac{1}{\rho} \mathbf{I} \right)^{-1} \mathbf{C}^H \quad (6)$$

where

$$\beta = \sqrt{\frac{E_{Tr}}{\text{tr}\left(\left(\mathbf{C}^H\mathbf{C} + \frac{1}{\rho}\mathbf{I}\right)^{-2}\mathbf{C}^H\mathbf{C}\right)}}. \quad (7)$$

The MMSE precoder is the optimal precoder to maximize the data rate for a single user. However, it uses the same scalar  $\beta^{-1}$  to scale all received symbols of multiple users. If the received symbols at different users have very different signal strengths due to different channel gains, the MMSE precoder is forced to equalize the channel gains, which results in a suboptimal performance. Besides, it minimizes the sum of mean squared errors of all users. If we would like to optimize the WSR, the weights (i.e.,  $\alpha_1$  and  $\alpha_2$  in (3)) cannot be considered in the MMSE precoder. Therefore, the MMSE precoder is not the optimal precoder to maximize the WSR with multiple users. Nevertheless, it is still a good choice due to its satisfying performance and simple, closed form (and therefore differentiable) solution.

### B. The WMMSE Precoder

Similar to the MMSE precoder, we define the error of user  $u$  as

$$e_u = \xi_u y_u - x_u, \quad (8)$$

where  $\xi_u$  is the scaling factor of user  $u$  (corresponding to  $\beta^{-1}$  in (4) but can be different for different users),  $y_u$  is the received symbol of user  $u$  (i.e., the  $u$ th element of  $\mathbf{y}$  in (1)) and  $x_u$  is the transmitted symbol of user  $u$  (i.e., the  $u$ th element of  $\mathbf{x}$  in (1)).

The WMMSE precoder considers the following problem

$$\begin{aligned} \min_{w_u, \mathbf{v}_u, \xi_u} \quad & \sum_{u=1}^U \alpha_u (w_u \mathbb{E}(e_u e_u^H) - \log w_u) \\ \text{s.t.} \quad & \sum_{u=1}^U \text{tr}(\mathbf{v}_u \mathbf{v}_u^H) \leq E_{Tr}, \end{aligned} \quad (9)$$

where  $w_u$  is the weight of the MSE of user  $u$ ,  $U$  is the number of users,  $\mathbf{v}_u$  is the precoding vector for user  $u$  of size  $M \times 1$  (i.e., the  $u$ th column of  $\mathbf{V}$  in (1)). It is proven that problem (9) is equivalent to the problem of WSR maximization (3) (when  $\Phi$  is fixed) in the sense that their optimal solutions of  $w_u$  and  $\mathbf{v}_u$  are the same when  $\xi_u$  is carefully selected for all users  $u$ .

Unfortunately, there is no closed-form solution to (9). Instead, Algorithm 1 is proposed to iteratively solve problem (9), where we define  $\mathbf{c}_u$  as the channel to user  $u$  of size  $1 \times M$  (i.e., the  $u$ th row of  $\mathbf{C}$ ),  $\mu^*$  is the Lagrange multiplier of the power constraint and is chosen such that the transmit power constraint in (9) is satisfied.

---

**Algorithm 1** Iterative WMMSE Precoder
 

---

 Initialize  $\mathbf{v}_u$ 
**repeat**
 $w'_u \leftarrow w_u$  for all users  $u$ 
 $\xi_u \leftarrow \left( \sum_{\nu=1}^U \mathbf{c}_u \mathbf{v}_\nu \mathbf{v}_\nu^H \mathbf{c}_u^H + 1/\rho \right)^{-1} \mathbf{c}_u \mathbf{v}_u$  for all users  $u$ 
 $w_u \leftarrow \left( 1 - \xi_u^H \mathbf{c}_u \mathbf{v}_u \right)^{-1}$  for all users  $u$ 
 $\mathbf{v}_u \leftarrow \alpha_u \left( \sum_{\nu=1}^U \alpha_\nu \mathbf{c}_\nu^H \xi_\nu w_\nu \xi_\nu^H \mathbf{c}_\nu + \mu^* \mathbf{I}_M \right)^{-1} \mathbf{c}_u^H \xi_u w_u$  for all users  $u$ 
**until**  $\left| \sum_{u=1}^U |w_u| - \sum_{u=1}^U |w'_u| \right| \leq \epsilon$ 


---

The WMMSE precoder is the optimal precoder to maximize the WSR. However, its complexity is considerably higher than the MMSE precoder. Besides, the iterative solution is not differentiable.

#### IV. PROPOSED FCN BASED APPROACH

##### A. The FCN Approach

An FCN consists of several two-dimensional convolutional layers, where each layer processes the feature maps of its preceding layer and extracts new feature maps from them. For example, in semantic segmentation, usually an RGB image is used as input for the network. The filters in the first layer operate on the three channels of the image and extract feature maps for the following convolutional layer. The filter kernels learned in the first layer are three-dimensional as they extract features from a three-dimensional input tensor. Each filter kernel generates one output feature map. The output of a semantic segmentation FCN in a certain task is a category for each pixel (e.g., road, car, pedestrian). The channels  $\mathbf{H}$  and  $\mathbf{G}$  reveal spatial correlation due to the short distance between RIS antennas. This property shows similarity to images, where adjacent pixels form an object, which can be captured by a two-dimensional convolutional filter. Encouraged by this analogy, we would like to compute  $\Phi$  with the FCN. The elementary unit of an RIS is an RIS antenna. Its features are the properties characterizing the wireless channels with respect to this RIS antenna, which will be defined later in Section IV-B.

As shown in Fig. 2(a), the input of the FCN is a three-dimensional array, where the first dimension is the feature map index  $k \in \{1, \dots, K\}$  with  $K$  the number of features, second and third dimensions are height  $h \in \{1, \dots, H\}$  and width  $w \in \{1, \dots, W\}$ , respectively. For



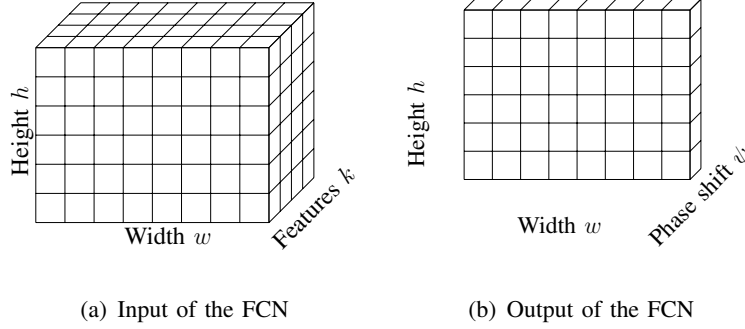


Fig. 2. Input and output format of the FCN. The input is a three-dimensional array with dimensions of channel features, height and width. Channel feature  $k$  of RIS antenna at position  $(h, w)$  is stored in coordinate  $(k, h, w)$ . The output is a two-dimensional array with dimensions of height and width. The phase shift of RIS antenna at position  $(h, w)$  is stored in coordinate  $(h, w)$ .

example, the value of feature map index  $k$  of the RIS antenna at position  $(h, w)$  is stored in coordinate  $(k, h, w)$  in the three-dimensional array. The output of the FCN is a two-dimensional array of the same height and width as the input, but with only one feature map being the phase shift of the antenna, as shown in Fig. 2(b).

Define  $\mathbf{Q}_\kappa$  as the  $\kappa$ th feature map of the output of a convolutional layer. It is computed as

$$\mathbf{Q}_\kappa = b_\kappa + \sum_{k=1}^K \mathbf{W}_{k\kappa} \star \mathbf{P}_k, \quad (10)$$

where  $b_\kappa$  is the bias of feature map with index  $\kappa$ ,  $\mathbf{W}_{k\kappa}$  is the filter kernel which takes feature map with index  $k$  as input and produces feature map with index  $\kappa$  as output,  $\mathbf{P}_k$  is the array of feature map with index  $k$  of the input,  $K$  is the number of feature maps of the input.

When applied in a straightforward manner, the cross-correlation operation makes the size of  $\mathbf{Q}_\kappa$  smaller than the size of  $\mathbf{P}_k$ . We use zero padding [36] such that the size of output equals the input size.

The size of the filters and the number of convolutional layers should be designed in such a way, that each output elementary unit has its receptive field <sup>2</sup> of the whole RIS. For example, if the RIS has the size of  $16 \times 16$ , a filter of size  $5 \times 5$  would have a receptive field with largest distance of  $(5 - 1)/2 = 2$  in each direction (i.e., left, right, up and down) in the input of the same layer. Therefore, we need 8 convolutional layers such that the output elementary unit in one corner has access to the input elementary unit in the opposite corner for an RIS size of  $16 \times 16$ .

<sup>2</sup>The region of the input that produces the output

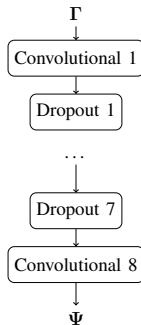


Fig. 3. Structure of the proposed FCN for phase shift optimization.

In order to prevent overfitting, we put a dropout layer [37] between each convolutional layer.

After all layers, the output of the FCN  $\Psi$  is the array of phase shifts of all RIS antennas of size  $H \times W$ . The structure of the proposed FCN is shown in Fig. 3. The computation of the FCN is denoted as  $\Psi = \Psi_{\theta}(\Gamma)$ , where  $\theta$  is the parameters of the FCN (i.e., all biases and filters of all layers),  $\Gamma$  is the input feature map,  $\Psi = (\psi_n)$  is the two-dimensional array with linearly addressed elements  $\psi_n, n = 1, \dots, N$ ,  $n$  is the index of the RIS antenna. For antenna at position  $(h, w)$ , we have  $n = H \cdot (h - 1) + w$ .

### B. Definition of Features

In problem (3),  $\mathbf{H}$  is assumed to be constant because both BS and RIS are stationary,  $\mathbf{G}$  and  $\mathbf{D}$  vary with the user positions and are required to compute  $\Phi$  and  $\mathbf{V}$ . We would like to interpret  $\mathbf{G}$  and  $\mathbf{D}$  as two feature maps with element index  $n$  referring to a certain RIS antenna. Accordingly, we can use our FCN. While each column of  $\mathbf{G}$  can be injectively mapped to each RIS antenna,  $\mathbf{D}$  is irrelevant to the RIS. Therefore, we define  $\mathbf{J} = \mathbf{D}\mathbf{H}^+$  and (1) becomes

$$\mathbf{y} = (\mathbf{G}\Phi + \mathbf{J})\mathbf{H}\mathbf{V}\mathbf{x} + \mathbf{n}. \quad (11)$$

Equation (11) can be interpreted as follows: the precoded signal  $\mathbf{V}\mathbf{x}$  is transmitted through channel  $\mathbf{H}$  to every RIS antenna and then through channel  $\mathbf{G}\Phi + \mathbf{J}$  to the users. Both  $\mathbf{G}$  and  $\mathbf{J}$  have  $N$  columns and their columns can be injectively mapped to the RIS antennas. Therefore, the features of an RIS element at position  $(w, h)$  can be defined as

$$\begin{aligned} \gamma_{wh} = (&|g_{1n}|, \arg(g_{1n}), |g_{2n}|, \arg(g_{2n}), \\ &|j_{1n}|, \arg(j_{1n}), |j_{2n}|, \arg(j_{2n})), \end{aligned} \quad (12)$$

where  $g_{k\kappa}$  is the element in row  $k$  and column  $\kappa$  of  $\mathbf{G}$ ,  $j_{k\kappa}$  is defined similarly to matrix  $\mathbf{J}$ . In this way, we use 8 features<sup>3</sup> to characterize the wireless channels with respect to each RIS antenna  $n$ , yielding the FCN input  $\mathbf{\Gamma} = (\mathbf{G}, \mathbf{J})$ .

### C. Objective Functions

Our objective function  $f$  in (3) is a function of channels  $\mathbf{G}$  and  $\mathbf{D}$ , RIS phase shifts  $\mathbf{\Phi}$  and BS precoding  $\mathbf{V}$ . When  $\mathbf{\Phi}$  is determined,  $\mathbf{V}$  can be computed with either MMSE precoder or WMMSE precoder as described in Section III, which are denoted as  $\mathbf{V}_{\text{MMSE}}(\mathbf{G}, \mathbf{D}, \mathbf{\Phi})$  and  $\mathbf{V}_{\text{WMMSE}}(\mathbf{G}, \mathbf{D}, \mathbf{\Phi})$ , respectively. It is to note that  $\mathbf{V}_{\text{MMSE}}$  is a differentiable function but  $\mathbf{V}_{\text{WMMSE}}$  is not differentiable.

Since  $f$  is a function of  $\mathbf{G}$ ,  $\mathbf{D}$ ,  $\mathbf{\Phi}$  and  $\mathbf{V}$ , we can express  $f$  as  $f(\mathbf{G}, \mathbf{D}, \mathbf{\Phi}, \mathbf{V})$ . Therefore, for MMSE precoding, the objective function is

$$f\left(\mathbf{G}, \mathbf{D}, \exp(j\Psi_{\theta}(\mathbf{G}, \mathbf{D})), \mathbf{V}_{\text{MMSE}}\left(\mathbf{G}, \mathbf{D}, \exp(j\Psi_{\theta}(\mathbf{G}, \mathbf{D}))\right)\right). \quad (13)$$

For WMMSE precoding, the objective function is

$$f\left(\mathbf{G}, \mathbf{D}, \exp(j\Psi_{\theta}(\mathbf{G}, \mathbf{D})), \mathbf{V}_{\text{WMMSE}}\left(\mathbf{G}, \mathbf{D}, \exp(j\Psi_{\bar{\theta}}(\mathbf{G}, \mathbf{D}))\right)\right). \quad (14)$$

Please note that  $\Psi_{\bar{\theta}}$  in (14) is untrainable, i.e.,  $\bar{\theta}$  is given and  $\Psi_{\bar{\theta}}(\mathbf{G}, \mathbf{D})$  is a constant. Therefore, we do not need to compute the derivative of  $\mathbf{V}_{\text{WMMSE}}$  since it does not contain trainable variable  $\theta$ .

We can then compute  $\frac{\partial f}{\partial \theta}$  to do gradient ascent to optimize  $\Psi_{\theta}$  such that  $f$  is maximized for both (13) and (14).

The compositions of the objective functions is illustrated in Fig. 4.

## V. IMPLEMENTATION AND TRAINING CONSIDERATIONS

As described in Section III, the MMSE precoder is simple and differentiable and the WMMSE precoder has a higher performance at the cost of complexity and nondifferentiability. During the

<sup>3</sup>As remarked in Section II, we assume two users in this work. If  $K$  users are considered, the number of features is  $4K$  and each feature is similarly defined as in (12).

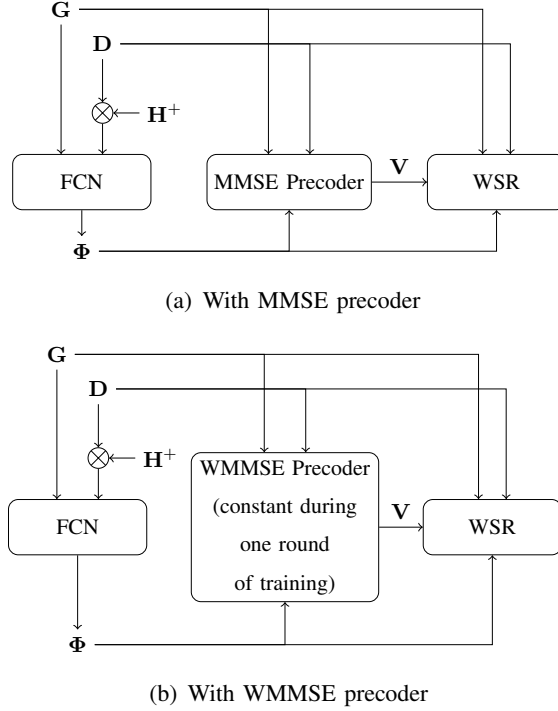


Fig. 4. Composition of the objective function. With the MMSE precoder, the input of the FCN  $\Gamma$  comprises  $\mathbf{G}$  and  $\mathbf{D}\mathbf{H}^+$ . The channel  $\mathbf{C}$  is determined by  $\mathbf{G}$ ,  $\mathbf{D}$  and  $\Phi$ , see (2). The MMSE precoding matrix  $\mathbf{V}$  is computed with (6). The WSR is determined by  $\mathbf{C}$  and  $\mathbf{V}$  together. With the WMMSE precoder, the structure of the objective function is similar, but  $\mathbf{V}$  is no more a function of  $\mathbf{G}$ ,  $\mathbf{D}$  and  $\Phi$ , but a constant which is updated periodically. Therefore, we do not compute the derivative of  $\mathbf{V}$ .

training, we apply the MMSE precoder and use (13) as the objective function in the first phase of training for a fast training and then switch to the WMMSE precoder and use (14) as the objective function to further improve the WSR in the second phase of training.

In the first phase, objective (13) is a function composition and its derivative can be computed with the chain rule. The MMSE precoding matrix is computed with the current phase shifts  $\Psi$ . On the contrary, in the second phase, the precoding matrix  $\mathbf{V}_{\text{WMMSE}}$  is nondifferentiable and is considered constant. Since  $\mathbf{V}_{\text{WMMSE}}$  changes with the channel, when  $\Psi$  changes because of the training,  $\mathbf{V}_{\text{WMMSE}}$  is no more valid. Therefore, we update  $\mathbf{V}_{\text{WMMSE}}$  every 10 epochs during training.

In the iterative WMMSE precoding algorithm (Algorithm 1), the initial precoding matrix is arbitrary subject to the transmit power constraint. The iteration is supposed to continue until convergence. In our training, however, it is desirable that (a) we only run a few iterations such that the training time is reasonable, (b) the updated precoding matrix is close to the precoding matrix

from the previous update, such that a drastic change is avoided and the training process is more fluent. With these considerations, we use the previous precoding matrix as the initial precoding matrix in the next update and run 5 iterations per update. In the first WMMSE precoding matrix update, the MMSE precoding matrix is applied. Although the WMMSE precoding matrix is not updated in real time as the MMSE precoding matrix, the change of the WMMSE is smooth and the training process is stable, as will be shown in Section VI.

We employ PyTorch [38] as the machine learning framework, which only supports real-valued inputs and parameters. Therefore, the channel features (12) use amplitude and phase to describe a complex channel gain. On the contrary, since PyTorch 1.9, complex numbers are supported in the objective function, which significantly reduces the complexity in implementation of (13) and (14). After implementation of the objective function, the gradient is computed with PyTorch's differentiation engine Autograd [38] without human intervention.

## VI. TRAINING AND EVALUATION RESULTS

In this section, we present the training and evaluation results. We apply a ray tracing channel simulator in an urban environment [39], where mobile users are supposed to have high demand for data rates. We generate channel from the BS to the RIS  $\mathbf{H}$ , channels from the RIS to the users  $\mathbf{G}$  and the direct channels  $\mathbf{D}$  of 5000 pairs of users, whose positions are randomly generated with a minimum distance of 2 meters between them. The scenario is shown in Fig. 5, where a line-of-sight (LoS) propagation path between BS and users is assumed to be unavailable due to the blockage by a building in the middle. A weak direct path is available through reflection on the building in the lower right corner. An RIS is equipped such that there are LoS propagation paths from BS to RIS and from RIS to users. A building behind the BS enables a strong reflection path from BS to RIS such that channel matrix  $\mathbf{H}$  has a rank higher<sup>4</sup> than 1.

Note that we assume the channel from BS to RIS  $\mathbf{H}$  is a constant, which holds because both positions of BS and RIS are fixed. However, it requires per-BS-RIS-pair channel measurement and training before deployment and when surrounding environment changes (e.g., a new building is built nearby), which should be plausible since per-cell optimization is a common practice [40]–[42].

<sup>4</sup>The rank of a matrix product is less than or equal to the rank of every matrix in the product. Since  $\mathbf{G}$  is the channel matrix to two users at different positions, it has a rank of 2.  $\Phi$  is a diagonal matrix and therefore has full rank. Therefore,  $\mathbf{H}$  has to have a rank higher than 1, otherwise we have to use the weak direct channel  $\mathbf{D}$ , which leads to a poor performance.

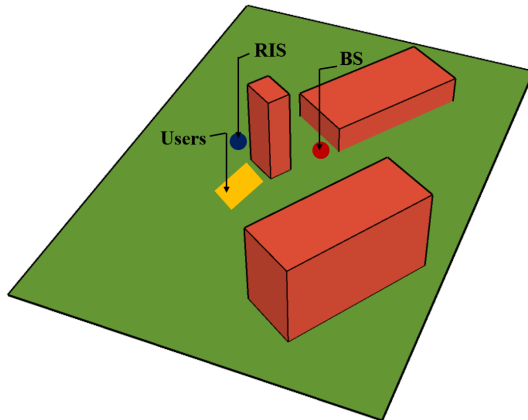


Fig. 5. The considered scenario. Positions of BS and RIS are given and positions of user pairs are generated randomly inside the yellow area. The LoS propagation path between BS and users is blocked by the high building in the middle. However, LoS propagation paths from BS to RIS and from RIS to users exist. A building behind the BS enables a strong reflection path from BS to RIS. A weak direct path is available through reflection on the building in the lower right corner.

The important parameters of scenario and model are presented in Table I. If multiple parameter values are considered, the default value is marked with a star (\*), which is always used without explicit specification.

Fig. 6 shows the improvement of the WSR with TSNR of  $10^{11}$  and user weights of (0.5, 0.5) in training. As explained in Section V, we first use the MMSE precoder to train the model for 4000 epochs, then switch to the WMMSE precoder for further training. It can be observed that the training has improved the WSR significantly with the MMSE precoder and the WMMSE precoder outperforms the MMSE precoder.

Fig. 7 shows the first 100 epochs of the training with the WMMSE precoder (i.e., epochs 4000 - 4100 in Fig. 6). Time points, where the precoding vectors are updated with the WMMSE precoder are marked with the red dots. At the beginning of the training with the WMMSE precoder, there is always a considerable performance improvement after the precoding vectors are updated. The performance is then improved slightly due to the FCN improvement. The improvement decreases as the training carries on until convergence.

To compare the proposed solution with other algorithms, we choose random RIS phase shifts and phase shifts optimized with the block coordinate descent (BCD) algorithm proposed as Algorithm 2 in [7] as two baselines. The number of iterations is increased from 100 in the original paper to 5000 due to the more complicated channel model in our paper (the original

TABLE I  
SCENARIO AND MODEL PARAMETERS

Parameter	Value
Number of BS antennas	9
RIS size	(16, 16)*, (32, 16), (32, 32)
Carrier frequency	5.8 GHz
Distance between adjacent antennas at BS	0.5 wave length
Distance between adjacent antennas at RIS	0.25 wave length
Transmit SNR	$10^{11}$ *, $1.1 \times 10^{11}$ , ... $10^{12}$
Weights of users	(0, 1), (0.25, 0.75), (0.5, 0.5)*, (0.75, 0.25), (1, 0)
Filter size	(5, 5) for RIS size of (16, 16), (13, 13) otherwise
Zero padding size	(2, 2) for RIS size of (16, 16), (6, 6) otherwise
Number of convolutional layers	8
Dropout rate	0.1 for RIS size of (16, 16), 0.35 otherwise
Training rate with MMSE precoder	$10^{-4}$
Epoches with MMSE precoder	4000
Training rate with WMMSE precoder	$2 \times 10^{-6}$
Updating interval with WMMSE precoder	10 Epoches
Epoches with WMMSE precoder	4000
Batch size	256
Optimizer	ADAM
Number of data samples in training set	5000
Number of data samples in testing set	1024

paper assumes i.i.d. Gaussian channels). All three algorithms use the WMMSE precoder. The FCN is evaluated with data that cannot be found in the training data set such that we can test the generality of the trained model.

Fig. 8 shows the rate regions of the three algorithms. Each curve is obtained with the user weights of (0, 1), (0.25, 0.75), (0.5, 0.5), (0.75, 0.25) and (1, 0) and every point is the average of performances of 1024 channel samples. We can see that both the BCD algorithm and the FCN improve the data rates of two users significantly from the random initialization. The FCN outperforms the BCD algorithm clearly. Besides, although training FCN and running BCD algorithm have time consumption in the same order of magnitude, training the FCN is only done once before the application. Testing FCN with 1024 channel samples takes merely a few seconds while running the BCD algorithm takes more than 4 hours with a 12-core CPU (channel samples are processed in parallel with the *parfor* loop in MATLAB). This makes the proposed

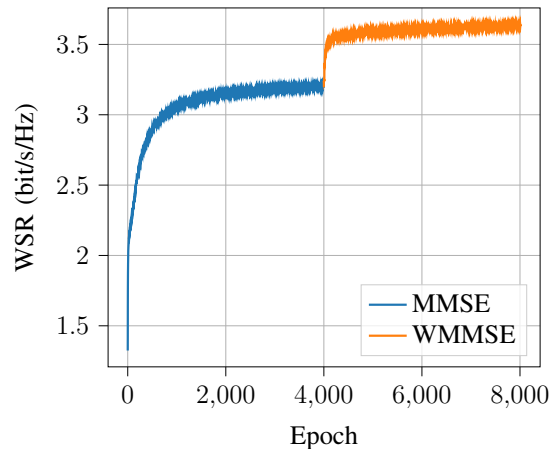


Fig. 6. Improvement of WSR in our proposed two-phase training protocol with pretraining with the MMSE precoder and “booster” training with the WMMSE precoder.

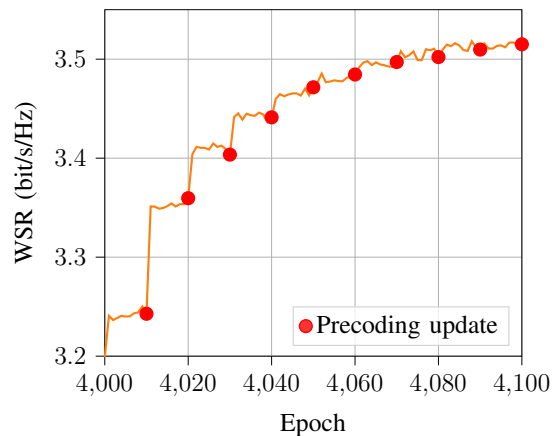


Fig. 7. Details to Fig. 6: Training with WMMSE precoder with update of precoding matrix every 10 epochs.

approach much more promising to be deployed in the near future for real-time applications given hardware with comparable performance as of today.

Fig. 9 shows the WSR with the same user weights (0.5, 0.5) and different TSNR. We can see that higher TSNR (i.e., transmit power) increases the data rate considerably and the RIS configured by the FCN outperforms random phase shifts and phase shifts optimized with the BCD algorithm for all tested TSNRs.

In the evaluation, we have obtained a WSR of 6.87 bit/s/Hz for  $\text{TSNR}=10^{11}$ . Compared to the WSR at the end of training (7.26 bit/s/Hz), the WSR in the evaluation is roughly 5% less than the WSR in the training, which suggests a low overfitting level and a good generalization



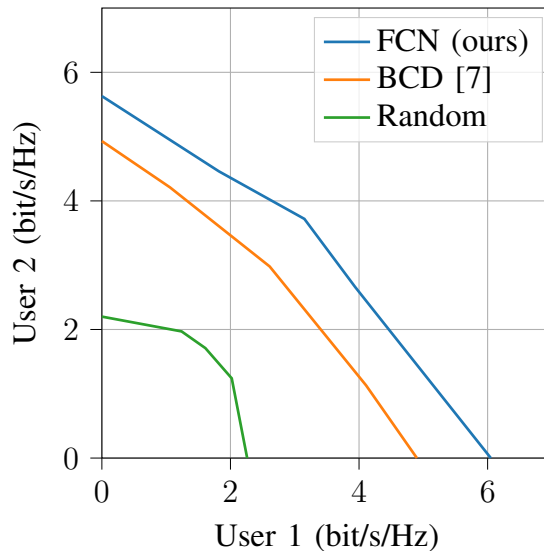


Fig. 8. Rate regions of baselines and proposed algorithm.

of the trained model.

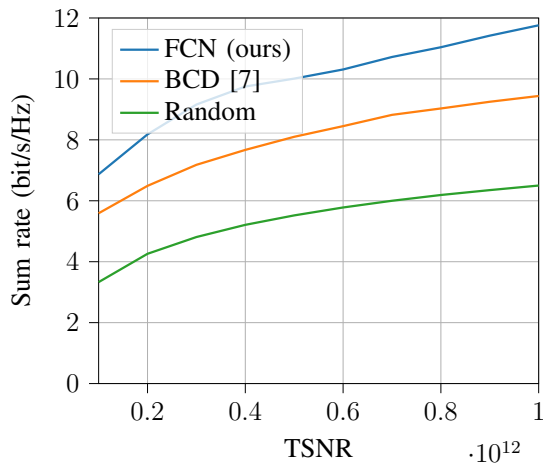


Fig. 9. Sum rates of baselines and proposed algorithm with different TSNRs.

Fig. 10 shows the sum rates of different approaches with different number of RIS antennas. It is to see that our proposed solution outperforms the two baselines with all tested numbers of antennas. Besides, although the FCN requires more training time due to bigger filter sizes (see TABLE I) and more RIS antennas, the evaluation of the FCN is within two minutes even for 1024 antennas on the author's two-year-old laptop with Intel's 8th generation i7 CPU (evaluation is run on the CPU) and 8 GB RAM, as shown in TABLE II. In contrast, the BCD algorithm

takes more than 3 days to optimize the RIS configuration with 1024 antennas on the server with a 12-core CPU, which makes it almost impractical for real-time deployment.

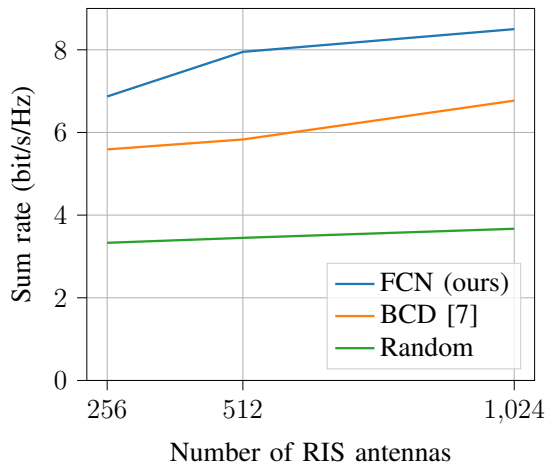


Fig. 10. Sum rates of baselines and proposed algorithm with different numbers of RIS antennas.

TABLE II  
TIME CONSUMPTION OF DIFFERENT APPROACHES

# of antennas	256	512	1024
Random	Seconds	Seconds	Seconds
BCD	5 hours	1 day	3 days
FCN training	5 hours	2 days	3 days
FCN evaluation	Seconds	Seconds	Minutes

Fig. 11 shows the empirical cumulative distribution function (ECDF) of the sum-rate with 256 RIS antennas, a TSNR of  $10^{11}$  and the user weights of (0.5, 0.5), where we can confirm the advantage of the proposed algorithm again. It is also to note that the ECDF of the proposed algorithm is flatter than the other two algorithms and the outage probability that the WSR is less than a given threshold is higher with the proposed algorithm than with the BCD algorithm proposed in [7], suggesting that the performance depends more heavily on the channels. The proposed algorithm only brings significantly advantage with favorable channels. Therefore, user selection is crucially important for the best performance, which remains an open problem.

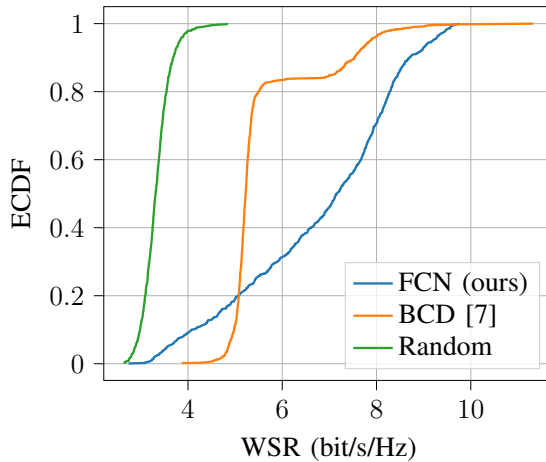


Fig. 11. ECDF of baselines and proposed algorithm.

## VII. CONCLUSIONS

We proposed an FCN based solution for spatial multiplexing enabled by a RIS in this paper. The FCN is a widely applied neural network architecture for computer vision but has not yet been used for RIS configuration. The rectangular shape of the RIS and the spatial correlation of channels on adjacent antennas of the RIS encourage us to apply the FCN to the RIS configuration. We use the simple and differentiable MMSE precoder for pretraining and the iterative and complex WMMSE precoder with periodically updated precoding vectors to fine-tune the model. A set of channel features is designed to include both cascaded channels via the RIS and the direct channel. We use a ray-tracing simulator to generate channel models with spatial correlation. Evaluation results show that the proposed solution achieves higher performance and also shows faster evaluation speed than the baselines. Therefore, it can be better scaled to a large number of antennas. The dropout layers between the convolutional layers of the FCN reduce overfitting.

It is shown that the WSR depends strongly on the wireless channels. As future works, it is desirable to find a criterion to optimally decide which users are selected to share the same resource block, which can significantly improve the average performance. Furthermore, more advanced techniques of interference management, such as nonorthogonal multiple access (NOMA) and rate splitting, can also be combined with RIS and may achieve a better performance than treating interference as noise.

The source code and channel data of this paper will be provided for public access if the article is accepted.

## ACKNOWLEDGEMENT

The results with random RIS phase shifts and with BCD algorithm are obtained with the open-source code generously shared by authors of [7] under [https://github.com/guohuayan/WSR\\_maximization\\_for\\_RIS\\_system](https://github.com/guohuayan/WSR_maximization_for_RIS_system).

The authors would like to thank Mrs. Xinyi Shan for providing the ray-tracing channel models.

## REFERENCES

- [1] S. V. Hum and J. Perruisseau-Carrier, “Reconfigurable reflectarrays and array lenses for dynamic antenna beam control: A review,” *IEEE Transactions on Antennas and Propagation*, vol. 62, no. 1, pp. 183–198, 2013.
- [2] C. Liaskos, S. Nie, A. Tsioliaridou, A. Pitsillides, S. Ioannidis, and I. Akyildiz, “A new wireless communication paradigm through software-controlled metasurfaces,” *IEEE Communications Magazine*, vol. 56, no. 9, pp. 162–169, 2018.
- [3] E. Björnson, L. Sanguinetti, H. Wymeersch, J. Hoydis, and T. L. Marzetta, “Massive MIMO is a reality—what is next?: Five promising research directions for antenna arrays,” *Digital Signal Processing*, vol. 94, pp. 3–20, 2019.
- [4] M. Di Renzo, A. Zappone, M. Debbah, M.-S. Alouini, C. Yuen, J. De Rosny, and S. Tretyakov, “Smart radio environments empowered by reconfigurable intelligent surfaces: How it works, state of research, and the road ahead,” *IEEE Journal on Selected Areas in Communications*, vol. 38, no. 11, pp. 2450–2525, 2020.
- [5] C. Huang, S. Hu, G. C. Alexandropoulos, A. Zappone, C. Yuen, R. Zhang, M. Di Renzo, and M. Debbah, “Holographic MIMO surfaces for 6G wireless networks: Opportunities, challenges, and trends,” *IEEE Wireless Communications*, vol. 27, no. 5, pp. 118–125, 2020.
- [6] C. Pan, H. Ren, K. Wang, W. Xu, M. Elkashlan, A. Nallanathan, and L. Hanzo, “Multicell MIMO communications relying on intelligent reflecting surfaces,” *IEEE Transactions on Wireless Communications*, vol. 19, no. 8, pp. 5218–5233, 2020.
- [7] H. Guo, Y.-C. Liang, J. Chen, and E. G. Larsson, “Weighted sum-rate maximization for reconfigurable intelligent surface aided wireless networks,” *IEEE Transactions on Wireless Communications*, vol. 19, no. 5, pp. 3064–3076, 2020.
- [8] Z. Zhang and L. Dai, “A joint precoding framework for wideband reconfigurable intelligent surface-aided cell-free network,” *IEEE Transactions on Signal Processing*, 2021.

- [9] C. Huang, A. Zappone, G. C. Alexandropoulos, M. Debbah, and C. Yuen, "Reconfigurable intelligent surfaces for energy efficiency in wireless communication," *IEEE Transactions on Wireless Communications*, vol. 18, no. 8, pp. 4157–4170, 2019.
- [10] K.-L. Besser and E. A. Jorswieck, "Reconfigurable intelligent surface phase hopping for ultra-reliable communications," *arXiv preprint arXiv:2107.11852*, 2021.
- [11] Z. Chu, W. Hao, P. Xiao, and J. Shi, "Intelligent reflecting surface aided multi-antenna secure transmission," *IEEE Wireless Communications Letters*, vol. 9, no. 1, pp. 108–112, 2019.
- [12] A. U. Makarfi, K. M. Rabie, O. Kaiwartya, K. Adhikari, X. Li, M. Quiroz-Castellanos, and R. Kharel, "Reconfigurable intelligent surfaces-enabled vehicular networks: A physical layer security perspective," *arXiv preprint arXiv:2004.11288*, 2020.
- [13] D. Mishra and H. Johansson, "Channel estimation and low-complexity beamforming design for passive intelligent surface assisted miso wireless energy transfer," in *ICASSP 2019-2019 IEEE International Conference on Acoustics, Speech and Signal Processing (ICASSP)*, IEEE, 2019, pp. 4659–4663.
- [14] Q. Wu and R. Zhang, "Weighted sum power maximization for intelligent reflecting surface aided swipt," *IEEE Wireless Communications Letters*, vol. 9, no. 5, pp. 586–590, 2019.
- [15] M. Joham, W. Utschick, and J. A. Nossek, "Linear Transmit Processing in MIMO Communications Systems," *IEEE Transactions on Signal Processing*, vol. 53, no. 8, pp. 2700–2712, 2005. DOI: 10.1109/TSP.2005.850331.
- [16] Q. Shi, M. Razaviyayn, Z.-Q. Luo, and C. He, "An iteratively weighted MMSE approach to distributed sum-utility maximization for a MIMO interfering broadcast channel," *IEEE Transactions on Signal Processing*, vol. 59, no. 9, pp. 4331–4340, 2011.
- [17] C. Huang, A. Zappone, M. Debbah, and C. Yuen, "Achievable rate maximization by passive intelligent mirrors," in *2018 IEEE International Conference on Acoustics, Speech and Signal Processing (ICASSP)*, IEEE, 2018, pp. 3714–3718.
- [18] N. S. Perović, L.-N. Tran, M. Di Renzo, and M. F. Flanagan, "On the maximum achievable sum-rate of the RIS-aided MIMO broadcast channel," *arXiv preprint arXiv:2110.01700*, 2021.
- [19] X. Liu, C. Sun, and E. A. Jorswieck, "Two-user SINR region for reconfigurable intelligent surface aided downlink channel," in *2021 IEEE International Conference on Communications Workshops (ICC Workshops)*, IEEE, 2021, pp. 1–6.

- [20] M. A. Elmoallamy, H. Zhang, R. Sultan, K. G. Seddik, L. Song, Z. Han, and Z. Han, "On Spatial Multiplexing Using Reconfigurable Intelligent Surfaces," *IEEE Wireless Communications Letters*, vol. 10, no. 2, pp. 226–230, 2021. DOI: 10.1109/LWC.2020.3025030. arXiv: 2009.07064.
- [21] Z. Li, M. Hua, Q. Wang, and Q. Song, "Weighted sum-rate maximization for multi-IRS aided cooperative transmission," *IEEE Wireless Communications Letters*, vol. 9, no. 10, pp. 1620–1624, 2020.
- [22] G. Zhou, C. Pan, H. Ren, K. Wang, and A. Nallanathan, "Intelligent reflecting surface aided multigroup multicast MISO communication systems," *IEEE Transactions on Signal Processing*, vol. 68, pp. 3236–3251, 2020.
- [23] K. Feng, Q. Wang, X. Li, and C.-K. Wen, "Deep reinforcement learning based intelligent reflecting surface optimization for MISO communication systems," *IEEE Wireless Communications Letters*, vol. 9, no. 5, pp. 745–749, 2020.
- [24] Y. Gao, C. Yong, Z. Xiong, D. Niyato, Y. Xiao, and J. Zhao, "Reconfigurable intelligent surface for MISO systems with proportional rate constraints," in *ICC 2020-2020 IEEE International Conference on Communications (ICC)*, IEEE, 2020, pp. 1–7.
- [25] D. Xu, X. Yu, and R. Schober, "Resource allocation for intelligent reflecting surface-assisted cognitive radio networks," in *2020 IEEE 21st International Workshop on Signal Processing Advances in Wireless Communications (SPAWC)*, IEEE, 2020, pp. 1–5.
- [26] Y. Yang, B. Zheng, S. Zhang, and R. Zhang, "Intelligent reflecting surface meets OFDM: Protocol design and rate maximization," *IEEE Transactions on Communications*, vol. 68, no. 7, pp. 4522–4535, 2020.
- [27] H. Li, R. Liu, M. Liy, Q. Liu, and X. Li, "IRS-enhanced wideband MU-MISO-OFDM communication systems," in *2020 IEEE Wireless Communications and Networking Conference (WCNC)*, IEEE, 2020, pp. 1–6.
- [28] G. Zhou, C. Pan, H. Ren, K. Wang, and A. Nallanathan, "A framework of robust transmission design for IRS-aided MISO communications with imperfect cascaded channels," *IEEE Transactions on Signal Processing*, vol. 68, pp. 5092–5106, 2020.
- [29] H. Gacanin and M. Di Renzo, "Wireless 2.0: Toward an intelligent radio environment empowered by reconfigurable meta-surfaces and artificial intelligence," *IEEE Vehicular Technology Magazine*, vol. 15, no. 4, pp. 74–82, 2020.

- [30] K. Yang, Y. Shi, Y. Zhou, Z. Yang, L. Fu, and W. Chen, “Federated machine learning for intelligent IoT via reconfigurable intelligent surface,” *IEEE Network*, vol. 34, no. 5, pp. 16–22, 2020.
- [31] J. Long, E. Shelhamer, and T. Darrell, “Fully convolutional networks for semantic segmentation,” in *Proceedings of the IEEE Conference on Computer Vision and Pattern Recognition (CVPR)*, 2015, pp. 3431–3440.
- [32] A. Pizzo, T. L. Marzetta, and L. Sanguinetti, “Spatially-stationary model for holographic MIMO small-scale fading,” *IEEE Journal on Selected Areas in Communications*, vol. 38, no. 9, pp. 1964–1979, 2020.
- [33] J. Dai, Y. Li, K. He, and J. Sun, “R-FCN: Object detection via region-based fully convolutional networks,” in *Advances in neural information processing systems*, 2016, pp. 379–387.
- [34] L. Wang, W. Ouyang, X. Wang, and H. Lu, “Visual tracking with fully convolutional networks,” in *Proceedings of the IEEE International Conference on Computer Vision (ICCV)*, 2015, pp. 3119–3127.
- [35] M. Honkala, D. Korpi, and J. M. Huttunen, “DeepRx: Fully convolutional deep learning receiver,” *IEEE Transactions on Wireless Communications*, vol. 20, no. 6, pp. 3925–3940, 2021.
- [36] S. Albawi, T. A. Mohammed, and S. Al-Zawi, “Understanding of a convolutional neural network,” in *2017 International Conference on Engineering and Technology (ICET)*, Ieee, 2017, pp. 1–6.
- [37] G. E. Hinton, N. Srivastava, A. Krizhevsky, I. Sutskever, and R. R. Salakhutdinov, “Improving neural networks by preventing co-adaptation of feature detectors,” *arXiv preprint arXiv:1207.0580*, 2012.
- [38] A. Paszke, S. Gross, F. Massa, A. Lerer, J. Bradbury, G. Chanan, T. Killeen, Z. Lin, N. Gimeshein, L. Antiga, A. Desmaison, A. Kopf, E. Yang, Z. DeVito, M. Raison, A. Tejani, S. Chilamkurthy, B. Steiner, L. Fang, J. Bai, and S. Chintala, “Pytorch: An imperative style, high-performance deep learning library,” in *Advances in Neural Information Processing Systems 32*, H. Wallach, H. Larochelle, A. Beygelzimer, F. d’Alché-Buc, E. Fox, and R. Garnett, Eds., Curran Associates, Inc., 2019, pp. 8024–8035.
- [39] D. He, B. Ai, K. Guan, L. Wang, Z. Zhong, and T. Kürner, “The design and applications of high-performance ray-tracing simulation platform for 5G and beyond wireless

- communications: A tutorial,” *IEEE Communications Surveys & Tutorials*, vol. 21, no. 1, pp. 10–27, 2018.
- [40] S. Shi, M. Schubert, N. Vucic, and H. Boche, “MMSE optimization with per-base-station power constraints for network MIMO systems,” in *2008 IEEE International Conference on Communications*, IEEE, 2008, pp. 4106–4110.
- [41] P. Baracca, F. Boccardi, V. Braun, and A. Tulino, “Base station selection and per-cell codebook optimization for CoMP with joint processing,” in *2012 IEEE 23rd International Symposium on Personal, Indoor and Mobile Radio Communications-(PIMRC)*, IEEE, 2012, pp. 2329–2334.
- [42] H. Eckhardt, S. Klein, and M. Gruber, “Vertical antenna tilt optimization for LTE base stations,” in *2011 IEEE 73rd Vehicular Technology Conference (VTC Spring)*, IEEE, 2011, pp. 1–5.